# Determination of a Micron-Scale Restricted Structure in a Perfluorinated Membrane from Time-Dependent Self-Diffusion Measurements

**T. Ohkubo,* K. Kidena, and A. Ohira**

*FC-Cubic, National Institute of Advanced Industrial Science and Technology (AIST), 2-41-6 Aomi, Koto-ku, Tokyo 135-0064, Japan*

*Received June 13, 2008; Revised Manuscript Received October 3, 2008*

ABSTRACT: We investigated the $^1$H time-dependent self-diffusion coefficients, $D_{eff}$, in perfluorinated membrane with low and high water contents (6% and 24%) at the temperature range from 233 to 323 K. The $D(\Delta_{eff})$ was measured as a function of the diffusion time, $\Delta_{eff}$, from 1 to 100 ms by field gradient NMR techniques. The oscillating gradient spin-echo sequence (OGSE) and the bipolar pulse longitudinal eddy current delay sequence (BPPLED) were employed to examine the $D(\Delta_{eff})$ of the short and long $\Delta_{eff}$. The results showed that the $^1$H self-diffusion coefficients were dependent on $\Delta_{eff}$ less than 2 ms due to restricted geometry and were constant beyond 3 ms. The tortuosity, $\alpha$, and surface-to-volume ratio of pore, *S*/*V*, for proton diffusion were estimated as geometrical parameters at each temperature. The values of *S*/*V* revealed the existence of micron-scale restricted structure compared with well-known nanometer-sized domain in perfluorinated membrane. Activation energy, $E_a$, of diffusion was also evaluated from the temperature dependence of diffusion at temperature above 263 K. The $E_a$ in the membrane and in the bulk water were almost the same at the temperature range above 263 K while it had some difference at lower temperature.

## 1. Introduction

Perfluorinated ion exchange membranes such as Nafion are currently the object of intense interest due to their potential use in fuel cells. Many studies of the proton conductivity were carried out to investigate its temperature and humidity dependence.[1−10] Microstructural models of perfluorinated membrane, in parallel, have been argued to clarify the proton transport mechanisms. So far, several excellent reviews have been published on the present understanding of the morphology and complex molecular-level proton transport mechanisms that determine the proton conductivity of perfluorinated membranes.[11−14]

The structural properties of perfluorinated membranes characterized by a microphase separation have been mainly studied using small-angle scattering of neutrons (SANS) and X-rays (SAXS). The existence of a small-angle scattering peak around $q = 2\pi/(4nm)$, where $q = 4\pi/\lambda \sin\theta$ with the scattering angle $2\theta$ and the X-ray or neutron wavelength $\lambda$, has been attributed to spherical reverse micelle of water domains, the so-called the Gierke model of a network of the spherical water domain connected by 1 nm channels.[15] Although the Gierke model was accepted widely, the further analytical research of SANS and SAXS data have been led the new aspects of water domain such as the Dreyfus model[16] with the micelles being organized on a diamond lattice. More recently, Schmidt-Rohr and Chen suggested the parallel cylindrical channels with networks by insight into the numerical simulation of SAXS profile.[17] These advanced models were based on the scattering data at the range of $q$ from 0.1 to 4 nm$^{-1}$. On the other hand, the scattering curve below $q = 0.1$ nm$^{-1}$ obtained by ultra-SAXS or ultra-SANS shows that the cavity structure of perfluorinated membrane is not just water domain but quite complex structure with some density variation at different scales from nanometers up to micrometers.[18] For instance, an elongated polymeric structure due to the aggregation of the ionomer chain was suggested as a new structural model.[19] However, little is known about long-range order (up to micrometer) structure in perfluorinated membrane when resolving the detailed transport mechanism related to proton conductivity.

The pulsed field gradient nuclear magnetic resonance (PFG NMR) is a commonly established method to measure the self-diffusion coefficients and is also used to probe the structure of restricted geometries on porous media.[20] The measurement of self-diffusion coefficients by NMR is based on the observation of spin migration (root-mean-square displacement) during the effective diffusion time, $\Delta_{eff}$. In the porous media the self-diffusion coefficients of confined fluid is not constant on $\Delta_{eff}$. If the $\Delta_{eff}$ allowed for the spin migration is brief enough, the effect of restricted geometry will have little impact on the measurement results, and the self-diffusion coefficient will closely reflect the intrinsic diffusion of bulk fluid. As the $\Delta_{eff}$ increases, spins interact more often with the physical restrictions; the self-diffusion coefficient gradually declines to an asymptotic value. From a series of experiments changing $\Delta_{eff}$ the unique geometrical information of porous media about the diffusion process, which is inaccessible to other techniques, can be extracted.

Several researchers have studied the self-diffusion coefficients of proton in perfluorinated membrane controlled water and methanol content.[3] However, as far as we know, the obvious difference of the self-diffusion coefficient on diffusion time has not been observed for perfluorinated membrane. The reason why the diffusion is independent of diffusion time that the detectable length scale of spin migration, $[D(\Delta_{eff})\Delta_{eff}]^{1/2}$, is too large as compared with the size of polymer cavity. Consequently, only tortuosity is observed as asymptotic value of $\Delta_{eff}$; the time-dependent diffusion is not observed.

In this study, we focused to probe the micron-scale porous structure in perfluorinated membrane through the observation of the time-dependent self-diffusion. Normally, the minimum diffusion time of PFG experiments is limited to 10 ms. This is not enough for perfluorinated membrane to observe the time-dependent self-diffusion. In order to measure the short diffusion length, slow diffusion coefficient or short diffusion time is required. Our strategy is to make use of the oscillating

* To whom correspondence should be addressed.

10.1021/ma801331e CCC: $40.75 
Published on Web 10/29/2008

gradient spin-echo technique[21,22] under low temperature. The oscillating gradient techniques make it possible to observe the self-diffusion coefficients with diffusion times less than 5 ms. Simultaneously, at the low temperature the self-diffusion coefficient of fluid is decreased. As a result, the self-diffusion coefficients within a short length scale will be detected. We report here some characteristic parameters for the perfluorinated membrane obtained by the time-dependent self-diffusion measurements.

## 2. Experimental Section

**2.1. Membrane Preparation.** Nafion N117 of DuPont (Wilmington, DE) was used as the perfluorinated membrane sample. The membrane was cut into thin 2.5 mm × 5 mm rectangular strips. Pieces of the cut membrane were immersed in 3% $H_2O_2$ aqueous solution at 353 K for 1 h and rinsed with deionized water at 353 K for 1 h. Next, the membranes were immersed in 1.0 M $H_2SO_4$ aqueous solution for 1 h and rinsed with deionized water at 353 K for 1 h. After removing surface water by filtration paper, eight cut pieces of membrane were put into glass tube (4 mm o.d., 40 mm height). Because of avoiding any heating effects, the drying process of membrane was not carried out.

To control the water content of membrane, we employed humidity chamber (Tabai Espec Corp, Osaka, Japan) and isopiestic equilibration of salt ($K_2SO_4$) method. Controlled conditions were two sets of the relative humidity, RH = 50% and RH = 97%, at room temperature. Equilibrium was achieved with a glass tube for 5 days at least. After reaching equilibrium, glass tubes were doubly sealed with silicone rubber plugs to avoid change of the water content during NMR measurements. The volume except for membrane in glass tube is ∼180 $mm^3$. It was confirmed that the sample weight did not change before and after NMR measurements.

The water contents, which were defined as (water weight)/(dry membrane weight), of a given membrane were determined by weighing the dried membrane after NMR measurements. The sample drying process was carried out such that the membranes in the glass tube were dried in a vacuum at 383 K for 24 h and were cooled in a desiccator. In order to prevent undesirable water absorption, the desiccator was filled with dry nitrogen gas. Then, the glass tube including membranes was sealed and weighed with a precision balance. The dry membrane weight was obtained by deducting the blank glass tube.

**2.2. $^1$H Self-Diffusion Coefficient Measurements.** All measurements were carried out on a JEOL ECA-500 at 11.7 T, narrow-bore NMR spectrometer equipped with maximum gradient strength of 1330 G/cm. The 4 mm o.d. glass tube including samples was sealed and inserted into a 5 mm o.d. standard NMR glass tube. In this study, we used two different pulse sequences as shown in Figure 1, which were applied to estimate self-diffusion coefficients with wide range of diffusion times. For short diffusion times from 1 to 3 ms, the oscillating gradient spin-echo (OGSE) pulse sequence[21] was employed. For long diffusion times of 30 ms or above, the bipolar pulse longitudinal eddy current delay (BPPLED) pulse sequence[23,24] was used with half-sine-shaped gradient pulses. It was slightly modified from the original sequences. These pulse sequences can mitigate the effect of the internal-field inhomogeneities, which are caused by the susceptibility contrast between the polymer matrix and the water filling the pores. For the porous media, it is essential to use these pulse sequences rather than the classical sequence of Tanner.[25]

The self-diffusion coefficients are measured by applying field gradients that produce a temporally and spatially varying phase structure on the spins across the sample. The strength and duration of applying field gradient change the spatial extent of the phase variations; they are rephased after diffusion time. The observable NMR signal, $E(g)$, is expressed as a function of spin dephasing (gradient strength and duration)

$$E(g) = E_0 \exp\left[-D\gamma^2 \int_0^t \{ \int_0^{t'} g(t'')\, dt''\}^2\, dt'\right] \equiv E_0 \exp(-Db) \quad (1)$$

where $D$ is the self-diffusion coefficients, $\gamma$ is the gyromagnetic ratio, $E_0$ is the NMR echo intensity without field gradient, and $g(t'')$ is the applied effective field gradient.[26] For these sequences the $\Delta_{eff}$ can be defined by comparison to the $b$ value calculation for a conventional pulsed gradient spin-echo experiment.[27] The $b$ value and $\Delta_{eff}$ of two pulse sequences are given in Table 1.

We have measured $E(g)$ for eight linearly spaced values of $g$ for a maximum value corresponding to the maximum signal attenuation of about 20%. It is assured that $E(g)$ is still in the Gaussian regime, and the self-diffusion coefficients can be obtained from eq 1 for BPPLED and OGSE sequences, respectively. This procedure was performed by a linear regression analysis on $\ln(E(g)/E(0))$ vs $b$.

We have used high field gradient strength compared with typical NMR probe. At the time, hardware problems originating from compatibility between a gradient coil and an amplifier led to erroneous diffusion coefficients. Therefore, we needed to check the actual gradient strength, which is the same condition as sample measurements. The gradient strength was carefully calibrated by estimation of $^2$H self-diffusion coefficient, $D = 2.054 \times 10^{-9}$ $m^2/s$ at 303 K, in deuterium oxide.[28] The $^1$H self-diffusion coefficient in water is not suitable for the purpose of the gradient calibration because signal attenuation is too large to test the maximum gradient strength. From the gyromagnetic ratio of $^2$H decrease by a factor of 0.154 for $^1$H, the gradient calibration using field gradient up to 600 G/cm is possible. The verification of pulse sequences was also performed by measuring the time-dependent self-diffusion of $^2$H in deuterium oxide. The constant self-diffusion coefficients on the diffusion time were obtained on $\Delta_{eff}$ from 1 to 100 ms, as shown in Figure 2. Accordingly, it was confirmed that the reliable time-dependent self-diffusion can be obtained by our equipments and the applied pulse sequences. With a good signal-to-noise ratio, the uncertainty in a given value of diffusion coefficient is about 5% at least.

The $^1$H self-diffusion coefficients of bulk water were also measured to define unrestricted diffusion at each temperature. The Milli-Q water was used as bulk water. To prevent freezing of liquid water at the temperature below melting point, supercooled water was made by putting into a small volume (∼0.05 $\mu$L) within capillary (0.14 mm i.d.). This contrivance to measure the supercooled water is the same as past NMR study of water.[29] The

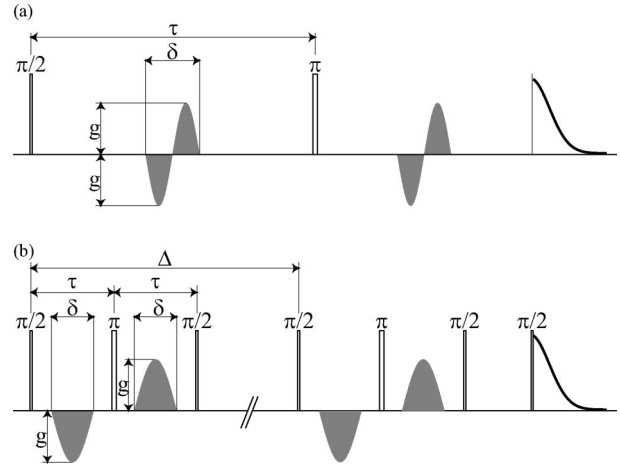


**Figure 1.** Two pulse sequences were employed to measure time-dependent self-diffusion on diffusion time, $\Delta_{eff}$, from 1 to 100 ms. (a) Oscillating gradient spin-echo sequence. The $\tau$ was fixed to 20 ms. The $\Delta_{eff}$ is adjusted in changing $\delta$. (b) Bipolar pulse longitudinal eddy current delay pulse sequence. The $\Delta_{eff}$ is adjusted in changing $\Delta$.

**Table 1. *b* Factor and Effective Diffusion Time, $\Delta_{eff}$, for Oscillating Gradient Spin-Echo Sequences,[21] OGSE, and Bipolar Pulse Longitudinal Eddy Current Delay Pulse Sequence[24] with Half-Sine-Shaped Gradients[a]**

| | $\Delta_{eff}$ | $b$ |
|---|---|---|
| OGSE | $0.375\delta$ | $3\gamma^2g^2\delta^3/4\pi^2$ |
| BPPLED | $\Delta - \tau/2 - \delta/8$ | $4\gamma^2g^2\delta^2(\Delta - \tau/2 - \delta/8)/\pi^2$ |

[a] BPPLED are listed. Referring to Figure 1, these pulse sequences have gradient strength, $g$, and duration, $\delta$. In the case of the BPPLED, $\Delta$ and $\tau$ are the spacing of gradients and the spacing between $\pi/2$ and $\pi$ pulse.

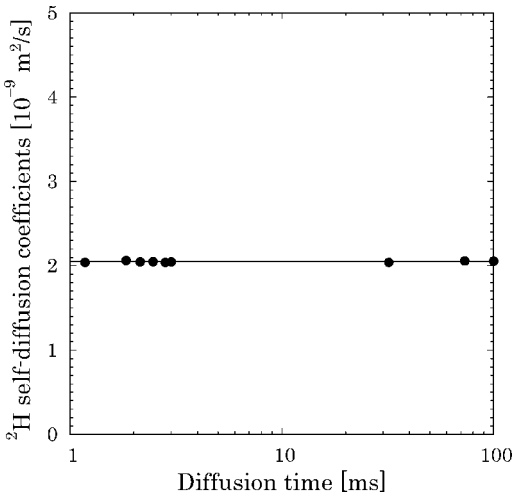


**Figure 2.** $^2$H self-diffusion coefficients on diffusion time from 1 to 100 ms in deuterium oxide was measured by use of maximum gradient up to 600 G/cm.

**Table 2. Measured Values of Self-Diffusion Coefficients, *D*, of Bulk Water at Temperatures from 248 to 323 K[a]**

| temperature (K) | $D$ ($10^{-9}$ m$^2$/s) |
|---|---|
| 233 | 0.343 |
| 248 | 0.708 |
| 263 | 1.08 |
| 278 | 2.25 |
| 293 | 2.68 |
| 308 | 3.70 |
| 323 | 5.02 |

[a] The value at 233 K is expected result from extrapolation of the fractional power law equation.[29]

measurements of bulk water were carried out by the BPPLED sequence with $\Delta_{eff} = 30$ ms.

Before NMR measurements, more than 1 h was allowed for the temperature to stabilize in all experiments.

## 3. Results and Discussion

The number of water molecules absorbed in the membrane per sulfonic acid group, $\lambda$, can be derived from absorbed amount of water at equivalent weight of N117 membrane (1100 g/equiv). The prepared membranes at RH = 97% and RH = 50% were 24% and 6% water contents; these correspond to $\lambda = 15$ and 4, respectively.

The measured self-diffusion coefficients of bulk water at 248, 263, 278, 293, 308, and 323 K are shown in Table 2. At all temperatures, the self-diffusion coefficients are well in agreement with reference data.[29,30] The NMR signal of liquid water disappeared about 237 K due to freezing of liquid water. On this account, the value expected from the extrapolation fractional power low, FPL, equation[29] was adopted as the self-diffusion coefficients of supercooled water at 233 K in Table 2. Figure 3 indicates $D(\Delta_{eff})$ of N117 membranes with 24% and 6% water content as a function of $\Delta_{eff}$ at 233, 248, 263, 278, 293, and 308 K. The self-diffusion coefficients at 323 and 338 K were

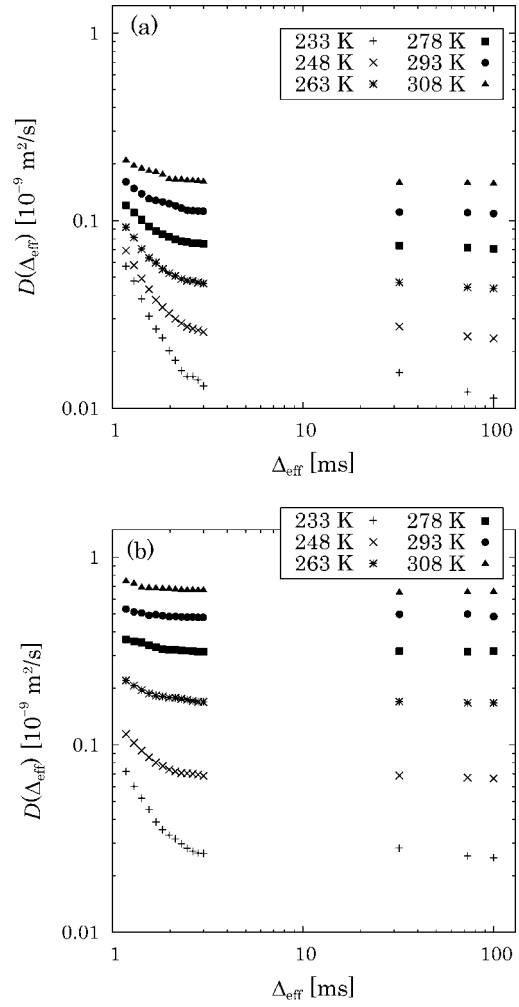


**Figure 3.** Measured self-diffusion coefficients, $D(\Delta_{eff})$, vs the diffusion time, $\Delta_{eff}$, in N117 membrane: (a) 6% water content; (b) 24% water content.

independent of the diffusion time and were not plotted in Figure 3. The $^1$H self-diffusion coefficients in N117 membrane clearly depended on $\Delta_{eff}$ less than 2 ms at least. These results demonstrated that there is restricted structure for N117 membrane on the length scale probed by this experiment. Especially the self-diffusion coefficients strongly depend on the diffusion time at lower temperature; the restricted diffusion may be enhanced due to the slow diffusion.

On the calculation of the self-diffusion coefficients, the signal attenuation with applied field gradient can be expressed by eq 1 as a single diffusion component. It is well-known that there are several kinds of proton species such as $SO_3^--H^+$, $H_3O^+$, and $H_2O$.[31] However, since the exchange process among these species occurs rapidly compared with the time scale of the NMR diffusion measurement, the obtained self-diffusion coefficients cannot be detected these species individually. We thus should regard the measured values as the weight average of these species.

An increase in the water content gives rise to fast diffusion as understood by comparison of Figure 3a,b regardless of the diffusion time. There is a large excess of $H_2O$ in N117 membrane with high water content; the proton can be exchanged rapidly for bulklike $H_2O$. This situation may lead to fast diffusion than the case of low water content. The self-diffusion coefficients for the long diffusion time as a function of water content have already been reported by Zawodzinski et al.;[2] these results are well in agreement with our data.

**Table 3. Estimated Values of Tortuosity, α, Surface-to-Volume Ratio, *S/V*, and Bulk Diffusion Coefficient, $D_0$, in N117 Membrane at Each Temperature[a]**

| water content (%) | temp (K) | $D_0$ ($10^{-9}$ m$^2$/s) | *S/V* ($\mu$m$^{-1}$) | α (au) |
|---|---|---|---|---|
| 6 | | | | |
| | 233 | 0.21 ± 0.01 | 5.9 ± 0.1 | 11.0 |
| | 248 | 0.22 ± 0.02 | 5.5 ± 0.1 | 14.5 |
| | 263 | 0.26 ± 0.02 | 4.7 ± 0.1 | 16.2 |
| | 278 | 0.29 ± 0.01 | 4.0 ± 0.02 | 17.6 |
| | 293 | 0.33 ± 0.02 | 3.3 ± 0.1 | 20.6 |
| | 308 | 0.34 ± 0.03 | 2.5 ± 0.2 | 19.5 |
| | 323 | | | 21.6 |
| | 338 | | | 19.4 |
| 24 | | | | |
| | 233 | 0.24 ± 0.02 | 5.2 ± 0.1 | 4.95 |
| | 248 | 0.29 ± 0.02 | 4.1 ± 0.02 | 5.17 |
| | 263 | 0.43 ± 0.02 | 2.6 ± 0.1 | 4.23 |
| | 278 | 0.56 ± 0.01 | 1.6 ± 0.1 | 3.95 |
| | 293 | 0.75 ± 0.05 | 1.1 ± 0.1 | 4.78 |
| | 308 | | | 4.50 |
| | 323 | | | 4.95 |
| | 338 | | | 4.68 |

[a] Errors reported here are the standard error of the fitting lines to experimental data.

**3.1. Tortuosity and Surface Area to Pore Volume Ratio.** NMR diffusion measurments are focused on monitoring the effects of geometric confinement on mean-square displacement. The mean displacement, $\langle z \rangle$, of fluid molecules undergoing unrestricted diffusion by random Brownian motion is given by

$$\langle z^2 \rangle = ([z(\Delta_{\text{eff}}) - z(0)]^2) = 2D_{\text{b}}\Delta_{\text{eff}} \tag{2}$$

where $z(\Delta_{\text{eff}})$ and $D_{\text{b}}$ are the position of the molecule at any diffusion time $\Delta_{\text{eff}}$. If the mean-squared displacement is short, i.e., short diffusion time, compared with diffusion space, the diffusion coefficient is insensitive to restrict with solid wall. As the diffusion time increases, the restriction of the solid wall becomes more effective for molecular diffusion. This situation led to time-dependent diffusion of fluid in porous media. At further diffusion time, the diffusion coefficient is constant any longer. This value reflect degree of tortuous structure of diffusion path

$$\alpha = \frac{\langle z^2 \rangle}{\langle z'^2 \rangle} = \frac{D_{\text{b}}}{D_\infty} \tag{3}$$

where $\langle z' \rangle$ and $D_\infty$ are the mean displacement undergoing restricted diffusion in porous media and the steady-state self-diffusion coefficient for long diffusion time, respectively. The self-diffusion coefficients for $\Delta_{\text{eff}} > 30$ ms were nearly independent of $\Delta_{\text{eff}}$ and seem to be approaching a constant value over the temperature range examined. When the root-mean-square displacement of spin was considered, the tortuosity, α, related to tortuous structure of diffusion path can be determined in this time scale:

$$\alpha = \frac{D_{\text{b}}}{D_\infty} \tag{4}$$

We regard $D_\infty$ as the values at $\Delta_{\text{eff}} = 100$ ms; α values for each sample at different temperatures were calculated as in Table 3.

The time-dependent diffusion is connected with surface-to-volume ratio, *S/V*, of pore space, which is assumed to be locally flat surface of pore wall and not a fractal, by Mitra et al.

$$D(\Delta_{\text{eff}}) = D_0\left(1 - \frac{4}{9\sqrt{\pi}}\frac{S}{V}\sqrt{D_0\Delta_{\text{eff}}}\right) \tag{5}$$

where $D_0$ is the bulk diffusion coefficient. To extract *S/V*, the Mitra equation[32] was applied to the $D(\Delta_{\text{eff}})$ for the short diffusion time less than 2 ms. The $D(\Delta_{\text{eff}})$ are plotted as a function of square root of $\Delta_{\text{eff}}$ and are fitted by the Mitra equation with the straight lines (see Figure 4). The *S/V* and $D_0$ are provided from the slope and the intercept of the straight lines and are given in Table 3. The values of $D_0$ obtained from the Mitra equation are quite lower than the $^1$H self-diffusion coefficients of bulk water. It is thought that the values of $D_0$ reflect the diffusion within the homogeneous network of cavities and so contain the transfer effect through the tortuous proton path. Rollet et al. have also obtained similar results based on the observation of the time-dependent self-diffusion of $N(CH_3)_4^+$ in N117 membrane immersed in $D_2O$.[33] However, we would like to emphasize that the observation of the $D(\Delta_{\text{eff}})$ of proton is the first result.

If we assume spherical pore with a diameter *a*, *S/V* corresponds to 6/*a*, where *a* is called "pore size". In our results, the pore size presumed from *S/V* is micrometer order and is quite large compared with hydrophilic domain size (nanometers size in the Gierke model). A feasible interpretation for the obtained *S/V* is the density fractionation of cavities resulting from heterogeneous distribution of cavity. The existence of heterogeneous cavity distribution may produce restricted wall for proton diffusion. Consequently, the cavity network has a specific size. The structural study for micron scale has been recently reported by ultrasmall angle scattering and AFM.[18,34] Kim et al. have also reported the possibility of superstructure originated from clustering of semicrystals.[35] Our results may supportd the result of these ultrasmall scattering studies.

The local diffusive behavior of proton in N117 membranes on a picosecond time scale was reported as a function of water content by use of quasi-elastic neutron scattering (QENS).[36] We can compare our results with the self-diffusion coefficient obtained from QENS. The QENS data as a function of *q* have been analyzed by interpreting with the confined spherical diffusion model at low *q* and the unbounded jump diffusion model at high *q*. The self-diffusion coefficients obtained from these models were plotted together with the results in this study at a similar temperature (see Figure 5). It is not surprising that the self-diffusion coefficients obtained from QENS are much greater than even the $D_0$ of NMR results. The self-diffusion coefficient on a picosecond time scale is not influenced by restricted geometry and reflects the degree of local motion. On the other hand, the behavior of diffusion on a millisecond time scale is distinct from that of picoseconds order and reflects the geometric character related to the cavities and the tortuosity.

Normally, the self-diffusion coefficient of fluid confined in porous media is gradually decreased with increasing diffusion time. However, it seems that the self-diffusion coefficients on pico- and millisecond time scales cannot connect with a smooth curved line as shown in Figure 5. And also, to compare diffusion behavior of the well-known cavity diameters with 1 and 4 nm,[15] which correspond to a *S/V* of 6.0 and 1.5 nm$^{-1}$, lines expected from the Mitra equation were also drawn in Figure 5. The time-dependent diffusion with cavity of a 4 nm diameter needs to cross at the $D_0$ at the time shorter than $10^{-8}$ at least. We thus suggest that there are two factors for determining the self-diffusion coefficient of long time scale: (1) the tortuous structure of the cavities within microseconds order of $\Delta_{\text{eff}}$ and (2) the structure of cavity network resulting from the heterogeneous distribution of cavities. The tortuous extent of (1) and the structure of cavity network of (2) are related to the $D_0$ and *S/V* in the Mitra equation, respectively. The QENS data fall in

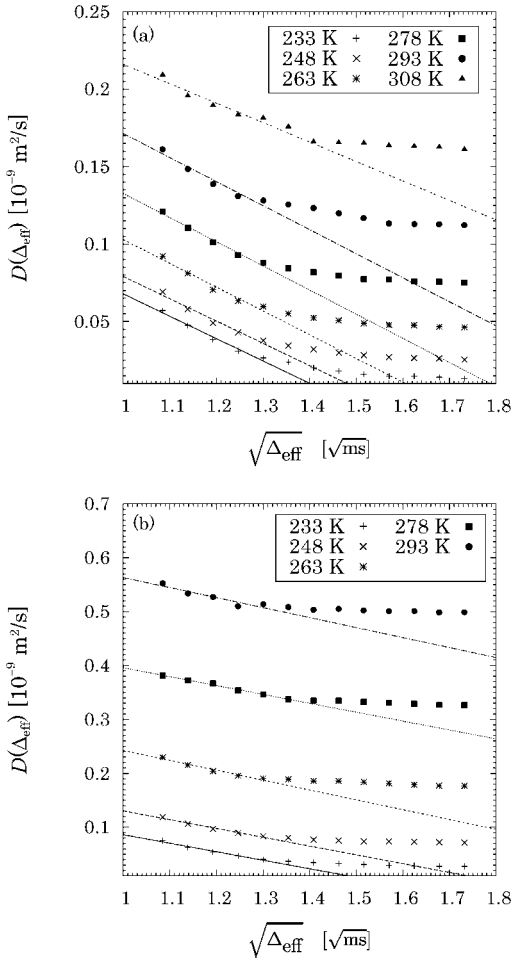


**Figure 4.** To extract *S*/*V*, the Mitra equation was applied to the time-dependent diffusion region for the short diffusion time less than 2 ms. Self-diffusion coefficients are plotted as a function of square root of diffusion time and are fitted with the straight line. The slope and the intercept of the straight lines correspond to *S*/*V* and $D_0$, respectively. (a) 6% water content; (b) 24% water content.

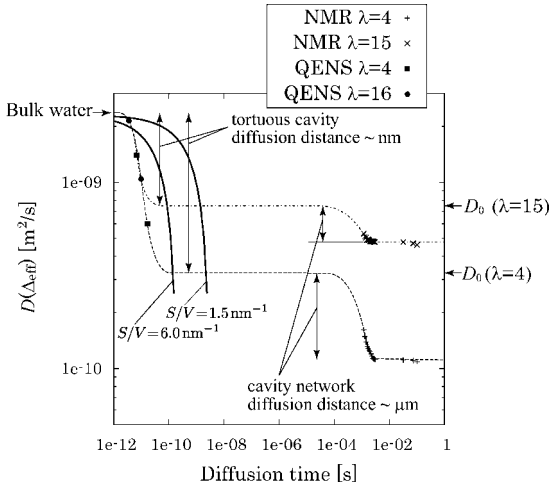


**Figure 5.** Relationship between the self-diffusion coefficients and the diffusion time over a wide range of time scale in N117 membrane. QENS data[36] at 295 K and NMR data at 293 K in this study were displayed with the similar number of water molecules per sulfonate, $\lambda$. Solid lines show expected behavior of time-dependent diffusion with cavity of 1 and 4 nm diameter corresponding to *S*/*V* of 6.0 and 1.5 nm$^{-1}$. Hypothetical behavior (dashed lines) of time-dependent self-diffusion were drawn based on QENS and NMR data.

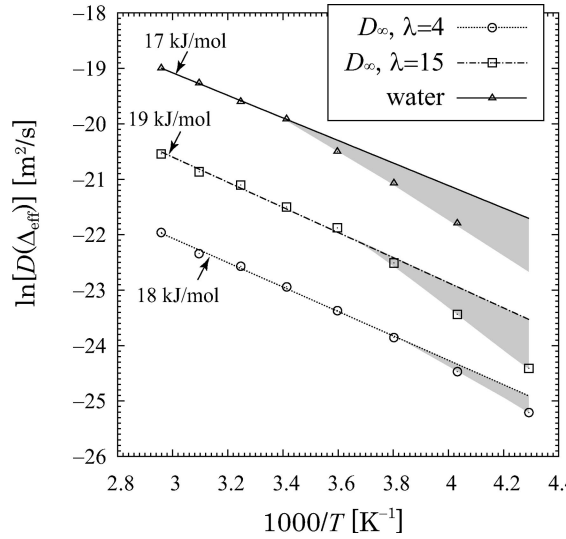


**Figure 6.** Arrhenius plots of the self-diffusion coefficients vs temperature. Activation energy was estimated from diffusion data at temperature range from 278 to 338 K for water and from 263 to 338 K for N117 membrane. The gray area at low temperature shows deviation from diffusion data expected from the activation energy.

shorter time than expected line. It may be presumed that *S*/*V* becomes larger for large *S* due to surface roughness. The time-dependent diffusion based on these putative behaviors was drawn with dashed lines in Figure 5. The $D(\Delta_{eff})$ at the range from $10^{-6}$ to $10^{-4}$ s time scale may not be a constant value, since the mixed contribution of factors (1) and (2) is expected. This aspect is still one of the plausible explanations to understand the macroscopic diffusion.

**3.2. Activation Energy of Diffusion.** Next we evaluated activation energy, $E_a$, from diffusion data. An Arrhenius behavior was supposed to calculate the $E_a$; the following equation was used:

$$D = A \exp\left(-\frac{E_a}{RT}\right) \tag{6}$$

where $D$ is the self-diffusion coefficients, $A$ is a constant, $R$ is the gas constant, and $T$ is the absolute temperature. In our study, the self-diffusion coefficients have been obtained based on two time scales (space scale), $D_0$ and $D_\infty$, where $D_\infty$ was the self-diffusion coefficient at $\Delta_{eff} = 100$ ms. We estimated $E_a$ from $D_\infty$.

Figure 6 shows the diffusion data as an Arrhenius plot. The values of $E_a$ for $D_\infty$ were obtained at the temperature range between 263 and 338 K. These were 18 and 19 kJ/mol for $\lambda =$ 4 and 15, respectively. The value of $E_a$ for bulk water also obtained at the temperature range between 293 and 338 K was 17 kJ/mol. The difference of $E_a$ between bulk water and N117 membranes was small. The fact means that the $^1$H in N117 membrane can diffuse like bulk water above 263 K.

The self-diffusion coefficients for bulk water below 278 K deviate from the line on $E_a = 17$ kJ/mol. Since the $E_a$ of bulk water (supercooled water) increased steeply with temperature decreasing below 273 K,[29] this is not the abnormal phenomenon. It is considered that the $E_a$ of the supercooled water was increased by the developed long-range hydrogen-bonded network at low temperature.[37] The deviation from $E_a$ at low temperature was also observed on N117 membranes. This tendency is more remarkable with high water content compared with the case of low water content. It is expected that the number of water molecules to form the developed long-range hydrogen-bonded network are insufficient in the case of lower water

content. Consequently, the temperature dependence of the self-diffusion coefficient with lower water contents was not changed even at 263 K or lower temperature. The similar tendency of $E_a$ that was increased at low temperature was reported with the conductivity data of N117 membrane. Thompson et al. explained from calorimetry measurements that the liquid water content in N117 membranes with high water content ($\lambda > 8$) is decreased by freezing at temperature below 273 K and only 6−7 water molecules per sulfonic group remain in the liquid state.[9] In our experiments, the existence of solid ice in the cavity with high water content gives lower self-diffusion coefficients because the diffusion of liquid water is obstructed by the ice phase. Therefore, we think that both the solid ice and the long-range hydrogen-bonded network (higher activation energy) of liquid water affect diffusion behavior at low temperature.

## 4. Conclusions

In this study, the time-dependent self-diffusion coefficients of proton in perfluorinated membrane with water content of 6% and 24% were measured by use of OGSE ($\Delta_{eff} < 3$ ms) and BPPLED ($\Delta_{eff} > 30$ ms) NMR sequences at the temperatures from 233 to 338 K. At temperatures below 293 K the self-diffusion coefficients were strongly dependent on the effective diffusion time until about 2 ms. To evaluate the geometric parameter of proton path, the Mitra equation was applied to the time-dependent self-diffusion. The obtained *S*/*V* proved the existence of the micron-scale restricted structure compared with cavity size in nanometers, and the bulk diffusion coefficients represented the value diffusion within the homogeneous network of cavities.

The activation energy of diffusion was estimated for the temperature range between 278 and 338 K. The results at temperatures above 278 K were almost the same to the bulk water regardless of the water content. At low temperature the temperature dependence of diffusion with $\lambda = 15$ was similar to that of supercooled water. On the other hand, that with $\lambda = 5$ was not much different from bulk water for temperatures above 278 K.

Finally, OGSE can provide a practical way to assess effects of restricted diffusion of $^1$H in polymer electrolyte membranes in the short diffusion time regime and may be useful in order to elucidate the proton transport mechanism.

**Acknowledgment.** This work was supported by New Energy Development Organization (NEDO), Japan. We gratefully acknowledge the NEDO project for financial support for this work.

## References and Notes

(1) Zawodzinski, T. A., Jr.; Derouin, C.; Radzinski, S.; Sherman, R. J.; Smith, V. T.; Springer, T. E.; Gottesfeld, S. *J. Electrochem. Soc.* **1993**, *140*, 1041.
(2) Zawodzinski, T. A., Jr.; Neeman, M.; Sillerud, L. O.; Gottesfeld, S. *J. Phys. Chem.* **1991**, *95*, 6040.
(3) Saito, M.; Tsuzuki, S.; Hayamizu, K.; Okada, T. *J. Phys. Chem. B* **2006**, *110*, 24410.
(4) Yeo, R. S. *J. Electrochem. Soc.* **1983**, *130*, 533.
(5) Uosaka, K.; Okazaki, K.; Kita, K. *J. Electroanal. Chem.* **1990**, *287*, 163.
(6) Zaluski, C. S.; Xu, G. *J. Electrochem. Soc.* **1994**, *141*, 448.
(7) Xu, G.; Pak, Y. S. *J. Electrochem. Soc.* **1992**, *139*, 2871.
(8) Cahan, B.; Wainright, J. *J. Electrochem. Soc.* **1993**, *140*, L185.
(9) Thompson, E. L.; Capehart, T. W.; Fuller, T. J.; Jorne, J. *J. Electrochem. Soc.* **2006**, *153*, A2351.
(10) Fontanella, J. J.; Edmondson, C. A.; Wintersgill, M. C.; Wu, Y.; Greenbaum, S. G. *Macromolecules* **1996**, *29*, 4951.
(11) Kreuer, K.; Paddison, S. J.; Spohr, E.; Schuster, M. *Chem. Rev.* **2004**, *104*, 4637.
(12) Elliott, J. A.; Paddison, S. J. *Phys. Chem. Chem. Phys.* **2007**, *9*, 2602.
(13) Mauritz, K. A.; Moore, R. B. *Chem. Rev.* **2004**, *104*, 4535.
(14) Wirguin, C. H. *J. Membr. Sci.* **1996**, *120*, 1.
(15) Hsu, W. Y.; Gierke, T. D. *J. Membr. Sci.* **1983**, *13*, 307.
(16) Dreyfus, B.; Gebel, G.; Aldebert, P.; Pineri, M.; Escoubés, M.; Thomas, M. *J. Phys. (Paris)* **1990**, *51*, 1341.
(17) Schmidt-Rohr, K.; Chen, Q. *Nat. Mater.* **2008**, *7*, 75.
(18) Gebel, G.; Lambard, G. *Macromolecules* **1997**, *30*, 7914.
(19) Rubatat, L.; Rollet, A. L.; Gebel, G.; Diat, O. *Macromolecules* **2002**, *35*, 4050.
(20) Callaghan, P. T. *Principles of Nuclear Magnetic Resonance Microscopy*; Oxford University Press: New York, 1991.
(21) Gross, B.; Kosfeld, R. *Messechnik* **1969**, *77*, 171.
(22) Schachter, M.; Does, M. D.; erson, A. W.; Gore, J. C. *J. Magn. Reson.* **2000**, *147*, 232.
(23) Cotts, R. M.; Hoch, M. J. R.; Sun, T.; Markert, J. T. *J. Magn. Reson.* **1989**, *83*, 252.
(24) Wu, D.; Chen, A.; Johnson, C. S. *J. Magn. Reson. A* **1995**, *115*, 260.
(25) Tanner, J. E. *J. Chem. Phys.* **1970**, *52*, 2523.
(26) Karlicek, R. F., Jr.; Lowe, I. J. *J. Magn. Reson.* **1980**, *37*, 75.
(27) Does, M. D.; Parsons, E. C.; Gore, J. C. *Magn. Reson. Med.* **2003**, *49*, 206.
(28) Woolf, L. A. *J. Chem. Soc., Faraday Trans. 1* **1975**, *71*, 1267.
(29) Price, W. S.; Ibe, H.; Arata, Y. *J. Phys. Chem. A* **1999**, *103*, 448.
(30) Woolf, L. A. *J. Chem. Soc., Faraday Trans. 1* **1975**, *71*, 784.
(31) Kreuer, K. D.; Paddison, S. J.; Spohr, E.; Shuster, M. *Chem. Rev.* **2004**, *104*, 4637.
(32) Mitra, P. P.; Sen, P. N.; Schwartz, L. M.; Le Doussal, P. *Phys. Rev. Lett.* **1992**, *68*, 3555.
(33) Rollet, A. L.; Simonin, J. P.; Turq, P.; Gebel, G.; Kahn, R.; Vandais, A.; Noël, J. P.; Malveau, C.; Canet, D. *J. Phys. Chem. B* **2001**, *105*, 4503.
(34) McLean, R. S.; Doyle, M.; Sauer, B. B. *Macromolecules* **2000**, *33*, 6541.
(35) Kim, M.; Glinka, C. J.; Grot, A.; Grot, W. G. *Macromolecules* **2006**, *39*, 4775.
(36) Pivovar, A. M.; Pivovar, B. S. *J. Phys. Chem. B* **2005**, *109*, 785.
(37) Prielmeier, F. X.; Lang, E. W.; Speedy, R. J.; Lüdemann, H.-D. *Ber. Bunsen-Ges. Phys. Chem.* **1988**, *92*, 1111.

MA801331E